Interaction of short x-ray pulses with low-Z x-ray optics materials at the LCLS free-electron laser

S. P. Hau-Riege,[1,*] R. A. London,[1] A. Graf,[1] S. L. Baker,[1] R. Soufli,[1] R. Sobierajski,[2,3] T. Burian,[4] J. Chalupsky,[4,5] L. Juha,[4] J. Gaudin,[6] J. Krzywinski,[7] S. Moeller,[7] M. Messerschmidt,[7] J. Bozek,[7] and C. Bostedt[7]

[1]*Lawrence Livermore National Laboratory, Livermore, California 94550, USA*
[2]*Institute of Physics PAS, Al. Lotników 32/46, PL-02-668 Warsaw, Poland*
[3]*FOM -Institute for Plasma Physics Rijnhuizen, NL-3430 BE Nieuwegein, The Netherlands*
[4]*Institute of Physics, Academy of Sciences of the Czech Republic, Na Slovance 2, 182 21 Prague 8, Czech Republic*
[5]*Faculty of Nuclear Science and Physical Engineering, Czech Technical University in Prague, Brehova 7, 115 19 Prague 1, Czech Republic*
[6]*European XFEL GmbH, Albert-Einstein-Ring 19, D-22761 Hamburg, Germany*
[7]*SLAC National Accelerator Laboratory, 2575 Sand Hill Road, Menlo Park, California 94025, USA*
*hauriege1@llnl.gov

Abstract: Materials used for hard x-ray-free-electron laser (XFEL) optics must withstand high-intensity x-ray pulses. The advent of the Linac Coherent Light Source has enabled us to expose candidate optical materials, such as bulk B_4C and SiC films, to 0.83 keV XFEL pulses with pulse energies between 1 µJ and 2 mJ to determine short-pulse hard x-ray damage thresholds. The fluence required for the onset of damage for single pulses is around the melt fluence and slightly lower for multiple pulses. We observed strong mechanical cracking in the materials, which may be due to the larger penetration depths of the hard x-rays.

©2010 Optical Society of America

OCIS codes: (340.0340) X-ray optics; (160.4670) Optical materials; (999.9999) X-ray free electron laser.

References and links

1. Y. Ding, A. Brachmann, F.-J. Decker, D. Dowell, P. Emma, J. Frisch, S. Gilevich, G. Hays, Ph. Hering, Z. Huang, R. Iverson, H. Loos, A. Miahnahri, H.-D. Nuhn, D. Ratner, J. Turner, J. Welch, W. White, and J. Wu, "Measurements and simulations of ultralow emittance and ultrashort electron beams in the linac coherent light source," Phys. Rev. Lett. **102**(25), 254801 (2009).
2. S. P. Hau-Riege, R. A. London, R. M. Bionta, D. Ryutov, R. Soufli, S. Bajt, M. A. McKernan, S. L. Baker, J. Krzywinski, R. Sobierajski, R. Nietubyc, D. Klinger, J. B. Pelka, M. Jurek, L. Juha, J. Chalupský, J. Cihelka, V. Hájková, A. Velyhan, J. Krása, K. Tiedtke, S. Toleikis, H. Wabnitz, M. Bergh, C. Caleman, and N. Timneanu, "Wavelength dependence of the damage threshold of inorganic materials under extreme-ultraviolet free-electron-laser irradiation," Appl. Phys. Lett. **95**(11), 111104 (2009).
3. S. P. Hau-Riege, R. A. London, R. M. Bionta, M. A. McKernan, S. L. Baker, J. Krzywinski, R. Sobierajski, R. Nietubyc, J. B. Pelka, M. Jurek, L. Juha, J. Chalupsky, J. Cihelka, V. Hajkova, A. Velyhan, J. Krasa, J. Kuba, K. Tiedtke, S. Toleikis, Th. Tschentscher, H. Wabnitz, M. Bergh, C. Caleman, K. Sokolowski-Tinten, N. Stojanovic, and U. Zastrau, "Damage threshold of inorganic solids under free-electron-laser irradiation at 32.5 nm wavelength," Appl. Phys. Lett. **90**(17), 173128 (2007).
4. J. Chalupský, V. Hájková, V. Altapova, T. Burian, A. J. Gleeson, L. Juha, M. Jurek, H. Sinn, M. Störmer, R. Sobierajski, K. Tiedtke, S. Toleikis, Th. Tschentscher, L. Vyšín, H. Wabnitz, and J. Gaudin, "Damage of amorphous carbon induced by soft x-ray femtosecond pulses above and below the critical angle," Appl. Phys. Lett. **95**(3), 031111 (2009).
5. S. P. Hau-Riege, R. M. Bionta, D. D. Ryutov, and J. Krzywinski, "Measurement of x-ray free-electron-laser pulse energies by photoluminescence in nitrogen gas," J. Appl. Phys. **103**(5), 053306 (2008).
6. S. P. Hau-Riege, R. M. Bionta, D. D. Ryutov, R. A. London, E. Ables, K. I. Kishiyama, S. Shen, M. A. McKernan, D. H. McMahon, M. Messerschmidt, J. Krzywinski, P. Stefan, J. Turner, and B. Ziaja, "Near-ultraviolet luminescence of N_2 irradiated by short X-ray pulses," Phys. Rev. Lett. **105**(4), 043003 (2010).
7. K. Tiedtke, A. Azima, N. von Bargen, L. Bittner, S. Bonfigt, S. Düsterer, B. Faatz, U. Frühling, M. Gensch, Ch. Gerth, N. Guerassimova, U. Hahn, T. Hans, M. Hesse, K. Honkavaar, U. Jastrow, P. Juranic, S. Kapitzki, B. Keitel, T. Kracht, M. Kuhlmann, W. B. Li, M. Martins, T. Nuñez, E. Plönjes, H. Redlin, E. L. Saldin, E. A. Schneidmiller, J. R. Schneider, S. Schreiber, N. Stojanovic, F. Tavella, S. Toleikis, R. Treusch, H. Weigelt, M.

Wellhöfer, H. Wabnitz, M. V. Yurkov, and J. Feldhaus, "The soft x-ray free-electron laser FLASH at DESY: beamlines, diagnostics and end-stations," N. J. Phys. **11**(2), 023029 (2009).

8. R. Soufli, S. L. Baker, J. C. Robinson, E. M. Gullikson, T. J. McCarville, M. J. Pivovaroff, P. Stefan, S. P. Hau-Riege, and R. Bionta, "Morphology, microstructure, stress and damage properties of thin film coatings for the LCLS x-ray mirrors," Proc. SPIE **7361**, 73610U (2009).

9. J. M. Liu, "Simple technique for measurements of pulsed Gaussian-beam spot sizes," Opt. Lett. **7**(5), 196–198 (1982).

10. J. Krzywinski, *et al*., *Focused beam properties in the High-Field AMO chamber*, unpublished.

11. B. L. Henke, E. M. Gullikson, and J. C. Davis, "X-ray interactions: Photoabsorption, scattering, transmission and reflection at E = 50–30000 eV, Z-1–92," At. Data Nucl. Data Tables **54**(2), 181–342 (1993).

12. NIST Chemistry WebBook, http://webbook.nist.gov/chemistry/

13. S. P. Hau-Riege, R. A. London, R. M. Bionta, R. Soufli, D. Ryutov, M. Shirk, S. L. Baker, P. M. Smith, and P. Nataraj, "Multiple pulse thermal damage thresholds of materials for x-ray free electron laser optics investigated with an ultraviolet laser," Appl. Phys. Lett. **93**(20), 201105 (2008).

14. D. C. Joy, *Monte-Carlo Modeling for Electron Microscopy and Microanalysis*, Oxford University Press, USA (1995).

15. B. Ziaja, R. A. London, and J. Hajdu, "Unified model of secondary electron cascades in diamond," J. Appl. Phys. **97**(6), 064905 (2005).

16. S. P. Hau-Riege, R. A. London, H. N. Chapman, and M. Bergh, "Soft-x-ray free-electron-laser interaction with materials," Phys. Rev. E Stat. Nonlin. Soft Matter Phys. **76**(4), 046403 (2007).

17. D. Broek, *Elementary Engineering Fracture Mechanics*, Springer, USA (1982).

1. Introduction

The world's first hard x-ray free electron laser (XFEL) – the Linac Coherent Light Source (LCLS) – has recently been built, providing high-brightness x-ray pulses with photon energies up to 8 keV [1]. The LCLS will be followed by similar XFEL facilities in Japan, the SPring8 Compact SASE Source (SCSS), and in Germany, the European XFEL. XFELs produce tunable, coherent, high-power radiation that will enable unique scientific research on ultrafast processes. At the same time, their unique output characteristics put severe requirements on the optics used to guide and shape the x-ray pulses and the detectors used to characterize them. This involves a new regime of radiation-matter interaction, which has been investigated in a series of experiments at the free electron laser in Hamburg (FLASH) at photon energies up to 177 eV [2–4]. The extreme ultraviolet (EUV) radiation available at FLASH interacts primarily with valence shell electrons and the penetration depth is much smaller than the beam diameter. The LCLS produces x rays ten to one hundred times higher in energy than FLASH. These x rays interacts primarily with inner shell electrons and the penetration depth is larger, comparable to the beam diameter. Therefore, the material damage mechanisms may be different for EUV and x-ray FELs. In this letter we report on experiments using 0.83 keV photons at LCLS. These experiments are of interest both as fundamental studies of ultra-short x-ray pulse interaction with matter and as practical studies relevant to the design of optics and detectors for XFEL facilities and experiments.

2. Description of experiment

In the usual operation of LCLS, 0.25 nC electron bunches, with a transverse emittance less than 1 μm, are injected into the last 1 km of the 3 km-long Stanford Linear Accelerator. After acceleration and compression, the bunches emerge with energies between 4.5 and 14.3 GeV, and are injected into a 132 m-long planar-hybrid undulator. The undulator is operated near the FEL collective instability, leading to the emission of high-brightness x-ray pulses that are linearly polarized with a horizontal electric-field vector. We performed the experiments at 0.83 keV, which was the lowest energy the LCLS at the time since damage effects are expected to be most pronounced at low x-ray energies. The LCLS pulse energies at the exit of the undulator varied between 1 and 2 mJ. The beam was attenuated in a nitrogen-filled gas cell and then transported to the Atomic, Molecular, and Optical Sciences (AMO) endstation. There it was focused to a diameter of 1 to 2 μm using a Kirkpatrick-Baez mirror pair. We positioned the samples 1 cm downstream of the focus where the footprint of the beam on the sample has an area at $1/e$ intensity level of ≈ 150 μm^2. We used a nitrogen-fluorescence detector to measure the absolute energy of each pulse [5,6]. The transmission of the beamline

from the nitrogen-fluorescence detector to the sample was 13%, measured by using an absolutely-calibrated gas energy monitor [7].

We exposed samples of bulk B_4C and thin SiC-films on Si substrates to the LCLS beam. These materials are of particular interest because bulk B_4C is used throughout the LCLS facility in protective stoppers, and SiC films are used as coatings for optical components. The bulk samples were fabricated using a hot-press process, leading to a grain size of a few μm, and polished to improve the surface roughness. Since B_4C has a high hardness, polishing is difficult. The surface showed multiple rip-outs, but in between the rip-outs the surface roughness was less than 0.5 nm. The SiC films were 1 μm thick and had 1.5 nm rms surface roughness, as measured by atomic force microscopy (AFM) in the 2 μm – 20 nm spatial range. They were deposited onto silicon wafer substrates using DC-magnetron sputtering, with the same deposition conditions as those used for the 50-nm-thick SiC reflective coatings on the LCLS hard x-ray mirrors. The deposition conditions are aimed towards SiC coatings with lower stress, at the expense of a slight increase in roughness [8]. The samples were exposed in rows of 20 to 30 single-shot exposures. For each exposure, we varied the gas attenuator pressure continuously from the start to the end of the row to cover a range of fluence. The XFEL was operated in an on-demand, single-pulse mode. Multiple-pulse exposures were also performed, but using a constant gas attenuator setting. In this case, the XFEL operated at 1 to 30 Hz, and the number of pulses per spot ranged from 1 to 10^4.
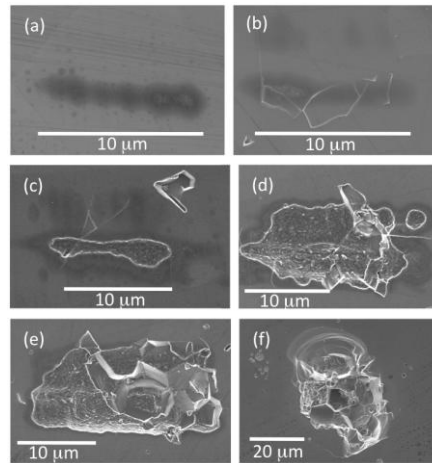

Fig. 1. SEM pictures of bulk B_4C exposed to single XFEL pulses at 0.83 keV and peak fluences of (a) 2.6, (b) 5.4, (c) 7.0, (d) 11.4, (e) 19.6, and (f) 90.5 J/cm^2.

3. Results

After the XFEL exposures, the samples were studied with a scanning electron microscope (SEM) and with an AFM. Figure 1 shows SEM pictures of bulk B_4C exposed to single 0.83 keV pulses of different pulse energies. We observed a strong dependence of the damage mechanism on the pulse energy. For low energies, surface roughening developed [Fig. 1(a)], and for somewhat higher energies, ablation and cracking occurred, [Fig. 1(b) and 1(c)]. For even higher pulse energies, substantial ablation and cracking was observed [Fig. 1(d)–1(f)].

We determined the threshold for damage from the energy dependence of the area of each damage spot as seen in the SEM images by a method described in [9]. Assuming the beam has a elliptical Gaussian profile, and that the beam interacts locally with the material, the damage area should scale linearly with the logarithm of the energy above a threshold value. The threshold energy for damage is given by the x intercept, and the slope of the curve gives the beam size. The data for B_4C are shown in Fig. 2. We see the expected linear behavior up to an energy of about 0.8 mJ, above which substantial cracking takes place. Applying this method to the low energy linear part of the curve, we obtain a beam area of 144 $μm^2$, in close

agreement with intensity measurements using beam imprints through focus [10]. From the intercept in Fig. 2, the damage threshold is 31 µJ, which corresponds to a fluence of 2.7 J/cm^2. This is close to the melt threshold of 2.2 to 2.6 J/cm^2, calculated from the x-ray absorption cross section [11] and the thermodynamic properties of B_4C [12].
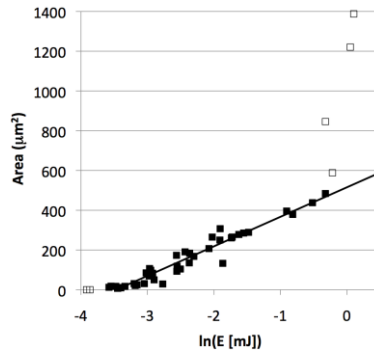

Fig. 2. Damage area as a function of the logarithm of the beam energy for bulk B_4C exposed at a photon energy of 0.83 keV. Only the data points plotted as solid squares are included in the linear fit since at high pulse energies (open squares) fracture in the sample leads to significantly larger damage areas.
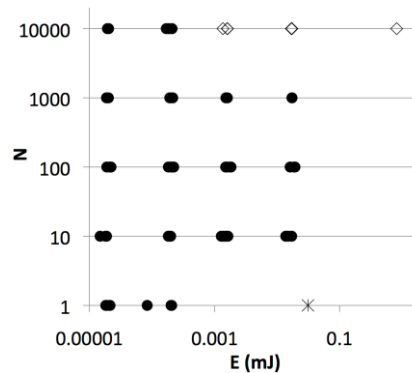
Fig. 3. Single and multiple-pulse damage threshold of bulk B_4C. Open symbols indicate observed surface damage, and closed symbols indicate that no damage was found in SEM images. The star symbol indicates single-pulse damage.

In previous experiments using a UV laser, it was found that the multiple-pulse damage threshold for B_4C lies below the single-pulse damage threshold [13]. We performed similar experiments on bulk B_4C at 0.83 keV, exposing the same spot up to 10^4 times. Each combination of pulse energy (E) and number of pulses (N) was repeated three times. The samples were then analyzed in the SEM. A map of the damage findings versus E and N (Fig. 3) indicates that for 10^4 pulses damage occurred below the single-pulse damage threshold. The spot is not visible in AFM, indicating that the surface change associated with the damage site is either very gradual toward the edge or the edge height is less than 0.1 nm. In the UV experiments on B_4C films, a gradual decrease of the damage threshold with increasing number of pulses was found [13], whereas in the x-ray experiments the transition occurred more abruptly between 10^3 and 10^4 pulses.
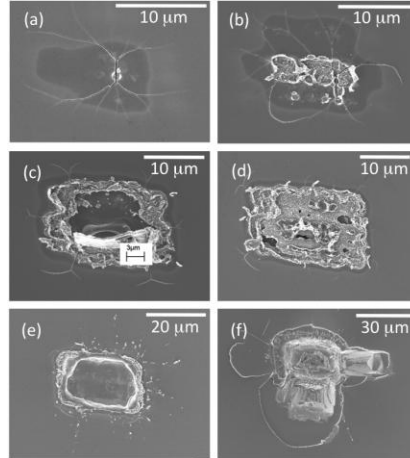
Fig. 4. SEM pictures of a SiC film exposed to single XFEL pulses at 0.83 keV and peak fluences of (a) 1.0, (b) 1.6, (c) 2.9, (d) 5.8, (e) 14.8, and (f) 57.5 J/cm^2.

Figure 4 shows SEM pictures of a 1 μm SiC film after exposure to the XFEL beam. The x-ray attenuation length in this case is 1.0 μm, comparable to the film thickness. The damage morphology is similar to the bulk B$_4$C case. Using the damage area versus pulse energy method, we obtain a beam area of 209 μm^2 and a damage threshold fluence of 0.62 J/cm^2. This fluence is somewhat lower than the melt threshold of 1.2 to 1.7 J/cm^2 for SiC. At the measured damage threshold, the fluence under the SiC layer is 0.30 J/cm^2, which is small compared to the melt threshold of bulk Si of 0.47 to 1.1 J/cm^2.

4. Discussion

We now compare the damage behavior observed on similar materials at lower photon energies at FLASH [2,3] with the present LCLS results. In both cases, we observed that the damage thresholds of bulk materials are somewhat above the melt threshold, whereas the damage threshold for films is below. For photon energies up to 92 eV, mechanical damage was not observed in B$_4$C and SiC, but only uniform ablation and occasionally extrusions. At 0.83 keV, we observe ablation at low pulse energy and, additionally, severe mechanical damage such as cracking at higher pulse energy. In both experiments, photons are absorbed through photo ionization, leading to the emission of energetic photoelectrons into the conduction band. In the soft x-ray case, the valence electrons are excited into the continuum, whereas inner-shell ionization dominates for the harder x-ray case, leading to the subsequent emission of Auger electrons on the time scale of a few femtoseconds. The range of the photo and Auger electrons is less than 20 nm in both cases [14], suggesting that initially, the heat stays localized, and that the difference in absorption processes should not have a strong direct effect on the damage mechanism. The energetic electrons interact with the bound electrons through electron impact ionization, and so thermalize within tens to hundreds of femtoseconds [15]. On the time scale of a picosecond, the electron gas equilibrates with the ions [16]. Then, on the timescale of nano- to microseconds, the heat is extracted from the interaction region through phonon-assisted heat diffusion. One of the major differences between the experiments with EUV and x rays is the aspect ratio of the interaction region of the FEL beam with the material. Assuming cold opacities, at 0.83 keV, the x-ray penetration depths are 1.6 μm in B$_4$C and 1.0 μm in SiC, whereas at 92 eV, the x-ray penetration depths are only 0.20 μm in B$_4$C and 0.22 μm in SiC [11]. In the hard x-ray case, a significantly larger amount of energy is deposited in the material for the same peak dose. For damage mechanisms that depend primarily on the energy per surface area, new damage processes may be activated. For example, the formation of cracks requires that the surface energy of the crack be smaller than the released volumetric strain energy. Since the heated volume is larger for hard x-rays, more strain energy is

available for mechanical deformation [17], which is in agreement with our experimental findings.

5. Summary

In summary, we exposed bulk B_4C and SiC film samples to LCLS XFEL pulses with pulse energies ranging from 1 μJ to 2 mJ. We found that the fluence required for the onset of damage in single pulses is comparable to the melt fluence. We find a slightly lower damage threshold for multiple pulses. Similar to the trends observed in experiments at longer wavelengths [2], the damage threshold is somewhat higher for bulk materials than for thin (μm-thick) films. Unlike in the longer-wavelength experiments, we observed strong mechanical cracking in the materials, which may be due to the larger penetration depths of the hard x-rays. Our results are in agreement with the main tenet for x-ray optics design to stay significantly below the melt threshold in order to prevent x-ray damage to optics.